PHYSICAL SCIENCES

UDC 519.63

Ulzi Uyanga, Bayaraa Taigyntuya. Finite element-based self-consistent formulation of the nonequilibrium green's function method for modeling quantum ballistic transport

Ulzi Uyanga,
Bayaraa Taigyntuya
Mongolia, Ulaanbaatar, MUST, School of Applied Sciences, Department of Mathematics

Abstract. *In this paper, we develop a computational strategy for analyzing nanoscale quantum transport under ballistic conditions by integrating a Green's function-based transport formalism with a spatial discretization method suitable for electrostatic modeling. The proposed method leverages the nonequilibrium Green's function (NEGF) approach to describe carrier behavior at the quantum level, while a mesh-based numerical scheme-specifically, the finite element technique is employed to solve the Poisson equation. This hybrid formulation enables accurate treatment of complex device geometries and naturally incorporates electrostatic boundary conditions without introducing artificial constraints. The simulation domain is based on a double-gate metal-oxide-semiconductor field-effect transistor (MOSFET), chosen to represent modern transistor structures. Key electronic properties, including the retarded Green's function, local carrier density, electrostatic potential distribution, and energy-resolved transmission, are computed self-consistently. To achieve convergence between the charge and potential profiles, the Newton-Raphson method is utilized. The numerical results demonstrate how potential distribution and quantum transport characteristics evolve across iterations and under different biasing conditions. In particular, the transmission spectrum and integrated Fermi functions provide insight into quantum tunneling and carrier injection phenomena in short-channel devices. These findings highlight the importance of coupled electrostatic-transport modeling in predicting quantum-scale device behavior and support the further development of simulation tools for next-generation semiconductor technologies.*

Keywords: *quantum-scale simulation, Green's function transport model, mesh-based electrostatics, self-consistent computation, advanced transistor modeling*

INTRODUCTION

As transistor dimensions continue to shrink into the nanometer regime, the demand for accurate simulation tools capable of handling quantum effects at this scale has significantly increased. This study focuses on modeling ballistic electron transport in a double-gate metal-oxide-semiconductor field-effect transistor (MOSFET) using the nonequilibrium Green's function (NEGF) framework [1], [2]. The NEGF approach provides a general and powerful method for investigating quantum transport phenomena in nanoscale devices.

Although the Schrödinger equation serves as the foundational equation for quantum transport theory, solving it directly for many-body systems remains a major computational

challenge. To overcome this, various methods have been developed-among which, the Green's function formalism is particularly well-suited for nanoelectronic applications. The NEGF method, widely used in quantum device simulations, was originally developed in the 1960s by researchers including Martin, Schwinger, Kadanoff, Baym, and Keldysh [3],[4].

Traditional formulations of NEGF are rooted in many-body perturbation theory (MBPT), which requires a deep understanding of advanced quantum mechanics. However, in this work, we adopt a simplified version of the formalism introduced by Supruyo Datta and others,

which emphasizes physical intuition over mathematical complexity.

The core of the NEGF method involves a self-consistent loop between the electrostatic (Poisson) equation and the quantum transport equation. The transport equation yields the electron density corresponding to a given potential, while the Poisson equation updates the electrostatic potential based on that density. These equations are iteratively solved until both quantities reach mutual convergence. To efficiently handle the two-dimensional device structure, an uncoupled mode space approximation is employed.

In this work, we implement a self-consistent numerical approach to model quantum transport, consisting of iterative steps described as follows:

1. Starting with an initial guess for the electrostatic potential, the Schrödinger equation is solved along the confinement direction to extract quantized subband energy levels.
2. These subband energies are then utilized to form the Hamiltonian matrix governing the transport characteristics of the device.
3. Using the constructed Hamiltonian, we compute the retarded Green's function, which in turn enables the evaluation of electron density and current flowing through the device terminals.
4. The calculated carrier density is then fed into the Poisson equation to update the potential profile, completing one iteration of the self-consistency loop.

Unlike prior works that commonly apply finite difference techniques for numerical discretization, this study adopts the finite element method (FEM). FEM provides notable advantages, such as its adaptability to irregular geometries and the ease of handling diverse boundary conditions. These features are particularly beneficial in quantum device simulations, where precise boundary representation is crucial.

In our Poisson equation formulation, homogeneous Neumann boundary conditions are imposed at both source and drain terminals. A notable strength of FEM is that it naturally

accommodates such boundary conditions-often referred to as floating boundaries-without requiring additional modifications or constraints in the model.

The simulation outputs include the self-consistently computed electrostatic potential, spatially resolved carrier density, and the integrated Fermi-Dirac distribution at the contacts.

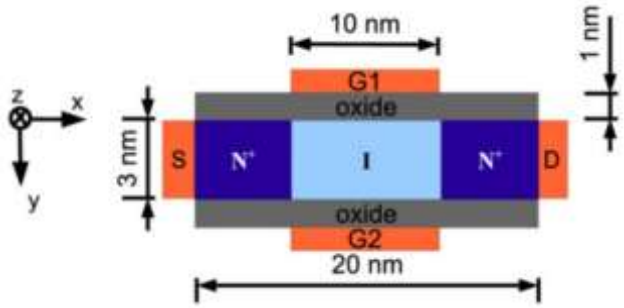

Figure 1: Geometry of the simulated double-gate MOSFET (adapted from Kurniawan, 2009)

The structure under investigation is a 2D double-gate MOSFET, chosen as the representative domain for simulation. The channel comprises source and drains regions, each 5 nm in length, separated by a 10 nm gate region. The layout, including the two gates, is shown in Figure 1.

I. THE NON-EQUILIBRIUM GREEN'S FUNCTION FORMALISM

We begin with the three-dimensional, time-independent Schrödinger equation:

$$-\frac{\hbar^2}{2m^*}\nabla^2\Psi(x,y,z)+\hat{U}\Psi(x,y,z)=E\Psi(x,y,z) \qquad (1)$$

Here, E denotes the eigenvalue of the Hamiltonian, $\Psi(x,y,z)$ is the quantum mechanical wavefunction, and $\hbar$ is the reduced Planck constant.

Assuming that the wavefunction behaves as a plane wave along the z-axis, i.e., $\Psi(x,y,z)=C\Phi(x,y)e^{ik_z z}$, we arrive at a reduced equation:

$$\begin{aligned}&-\frac{\hbar^2}{2m_x^*}\frac{\partial^2\Phi(x,y)}{\partial x^2}-\frac{\hbar^2}{2m_y^*}\frac{\partial^2\Phi(x,y)}{\partial y^2}+U(x,y)\Phi(x,y)\\&=\left(E-E_{k_z}\right)\Phi(x,y)\\&=E_1\Phi(x,y)\end{aligned} \qquad (2)$$

where E_1 is the transverse energy component, and E_{k_2} corresponds to the kinetic energy along z. The variables m_x^* and m_y^* are the effective masses along x and y, respectively, and U(x, y) represents the potential energy landscape in the transverse plane [10].

To proceed, we express $\Phi(x,y)$ as a superposition of mode (or subband) functions:

$$\Phi(x,y)=\sum_n \phi^n(x)\xi^n(y;x) \qquad (3)$$

Each term $\xi^n(y,x)$ solves the Schrödinger equation in a transverse slice at a fixed $x=x_0$

$$-\frac{\hbar^2}{2m_y^*}\frac{d^2\xi^n(y;x_0)}{dy^2}+U(y;x_0)\xi^n(y;x_0) = E_{\text{sub}}^n(x_0)\xi^n(y;x_0) \qquad (4)$$

Substituting (3) into (4), multiplying through by $\xi^m(y,x)$, and integrating over y, we apply the uncoupled mode approximation-assuming the mode shapes remain unchanged across x and do not interact [6] and obtain the 1D Schrödinger equation in the transport direction:

$$-\frac{\hbar^2}{2m_x^*}\frac{d^2\phi^m(x)}{dx^2}+E_{\text{sub}}^m(x)\phi^m(x)=E_1\phi^m(x) \qquad (5)$$

where $E_{\text{sub}}^m(x)$ is the energy associated with the m^{th} mode along x, determined from (4).

For a fixed mode and energy E, the retarded Green's function is formulated as:

$$G^m(E)=\left(ES^m-H_{mm}-\Sigma_S^m(E)-\Sigma_D^m(E)\right)^{-1} \qquad (6)$$

Here, H_{mm} and S^m are the mode Hamiltonian and overlap matrices, respectively. $\Sigma_S^m(E)$ and $\Sigma_D^m(E)$ are self-energy matrices capturing interactions with the source and drain terminals. In the absence of scattering (ballistic regime), these self-energies are computed from boundary contributions in the variational formulation [7].

Using the finite element method (FEM), the Hamiltonian matrix elements are computed via:

$$H_{ij}=\int\left(\alpha\frac{\partial N_i}{\partial k}\frac{\partial N_j}{\partial k}+\beta N_iN_j\right)dk \qquad (7)$$

and the corresponding elements of the overlap matrix are given by:

$$S_{ij}=\int\left(N_iN_j\right)dk \qquad (8)$$

Here, N_i and N_j denote the FEM basis functions. The integration variable dk is either dx or dy, depending on context. The coefficients α and β vary with the Hamiltonian under consideration:

$$\alpha = \frac{\hbar^2}{2m_y^*}, \beta = U \qquad (9)$$

$$\alpha = \frac{\hbar^2}{2m_x^*}, \beta = E_{\text{sub}}^m \qquad (10)$$

To compute carrier statistics, the spectral density matrix from contact L is defined as:

$$A_L^m(E) = G^m(E)\Gamma_L^m(E)G^{m\dagger}(E) \qquad (11)$$

with the broadening matrix

$$\Gamma_L^m(E) = i\left(\Sigma_L^m(E) - \Sigma_L^{m^\dagger}(E)\right) \qquad (12)$$

The 1D carrier density is derived by integrating over energy and considering contributions from both contacts:

$$n_{1D}^m(x) = \frac{1}{\pi h_x}\int_{-\infty}^{\infty}\left(f_S(\mu_S - E)A_S^m(E)S^m + f_D(\mu_D - E)A_D^m(E)S^m\right)dE$$

Here, μ_S and μ_D are the source and drain chemical potentials, and h_x is the spatial discretization step in x. The distribution function accounting for longitudinal integration is:

$$f_{1D}(\mu, E) = 2\left(\frac{2m_z^* k_B T}{\pi\hbar^2}\right)^{1/2} \mathrm{F}_{-1/2}\left(\frac{\mu - E}{k_B T}\right)$$

The 2D density is reconstructed as:

$$n_{2D}^m(x,y) = n_{1D}^m\left|\xi^m(y;x)\right|^2$$

Transmission probability through the channel is:

$$T^m(E) = \mathrm{Trace}\left(\Gamma_S^m(E)G^m(E)\Gamma_D^m(E)G^{m^\dagger}(E)\right)$$

The distribution of electron density within the device is inherently linked to the electrostatic potential V. To determine the potential profile, we employ a self-consistent approach by coupling it with the Poisson equation:

$$\nabla\cdot(\varepsilon_r\nabla V) = -\frac{q}{T_0}(N_D^+ - n_{2D})$$

The formulation of the self-energy matrix, derived via the finite element method, can be found in [7]:

$$\left[\Sigma_L\right]_{ij} = -\frac{\hbar^2}{2m_L^*} ik_L \delta_{i\in\gamma_L} \delta_{j\in\gamma_L} \qquad (13)$$

Here, the index L LLL refers to the contact region-either the source or the drain-while γ_j denotes nodes situated at the boundary between the contact and the active device region. The wavevector k_L is obtained from the dispersion relation:

$$E - E_{\text{sub}}^m(j) = \frac{\hbar^2 k_L^2}{2m_L^*}. \qquad (14)$$

2.1. Nonlinear Poisson Equation

For an n -type semiconductor, the electrostatic potential V is governed by the following form of the Poisson equation:

$$\nabla \cdot (\varepsilon_r \nabla V) = -\frac{q}{\mathrm{T}_0}(N_D^+ - n_{2D})$$

Here, $V = -U/q$ with U denoting the potential energy in joules and qqq representing the elementary charge. Here, N_D^+ corresponds to the concentration of ionized donor impurities, ε_r is the relative permittivity of the material, and ε_0 is the vacuum permittivity.

The electrostatic potential and carrier density are computed in a mutually consistent manner. The nonlinear Poisson equation is addressed using the method outlined in [9], which applies the Newton-Raphson iterative scheme to achieve convergence.

Following the computation of the electron density, the quasi-Fermi level is subsequently evaluated.

$$F_n = U_{\text{old}} + k_B T \mathrm{F}_{1/2}^{-1}\left(\frac{n_{2D}}{N_C}\right)$$

where n_{2D} denotes the two-dimensional carrier concentration and N_C represents the effective density of states in the conduction band. The function $\mathrm{F}_{1/2}^{-1}$ refers to the inverse of the complete Fermi-Dirac integral of order 1/2, as detailed in [10].

The electron density can also be expressed in terms of the quasi-Fermi level via:

$$n_{2D} = N_C \mathrm{F}_{1/2}\left(\frac{F_n - U_{new}}{k_B T}\right).$$

Upon determining F_n, it is incorporated into the nonlinear Poisson formulation:

$$-\nabla\cdot\left(\mathrm{T}_r\nabla U_{\text{new}}\right)=\frac{q^2N_C}{\mathrm{T}_0}\left(\mathrm{F}_{1/2}\left(\frac{F_n-U_{\text{new}}}{k_BT}\right)-\frac{N_D^+}{N_C}\right),$$

where $\mathrm{F}_{1/2}$ is again the complete Fermi-Dirac integral of order 1/2, as described in [15].

In order to formulate the linearized system required for the Newton-Raphson iteration, we begin by applying the finite element method (FEM) to discretize the nonlinear Poisson equation. The weak (variational) form of the governing equation is given by:

$$\int_\Omega\left[-\nabla\cdot\left(\mathrm{T}_r\nabla u\right)v-\frac{q^2N_C}{\mathrm{T}_0}\left(\mathrm{F}_{1/2}\left(\frac{F_n-u}{k_BT}\right)-\frac{N_D^+}{N_C}\right)v\right]d\Omega=0.$$

To proceed, we employ piecewise linear basis functions to approximate the electrostatic potential. Using the standard Galerkin approach, we let

$$u=\sum_{j=1}^{N}U_jN_j\ \text{and}\ v=N_i$$

which leads to a set of nonlinear algebraic equations for the coefficients $U_1,...,U_N$:

$$f_i\left(U_1,\ldots,U_N\right)=\int_\Omega-\nabla\cdot\left(\mathrm{T}_r\nabla\left(\sum_{j=1}^{N}U_jN_j\right)\right)N_i-$$

$$\frac{q^2N_C}{\mathrm{T}_0}\left(\mathrm{F}_{1/2}\left(\frac{F_n-\sum_{s=1}^{N}U_sN_s}{k_BT}\right)-\frac{N_D^+}{N_C}\right)N_i\,d\Omega=0,$$

for each $i=1,...,N.$.

To solve this nonlinear system, we employ the Newton-Raphson method, which at the k-th iteration yields the linear system:

$$\sum_{j=1}^{N}\frac{\partial}{\partial U_j}f_i\left(U_1^k,\ldots,U_N^k\right)\delta U_j=-f_i\left(U_1^k,\ldots,U_N^k\right),$$

for $i=1,\ldots,N,$ followed by the update rule:

$$U_j^{k+1}=U_j^k+w\delta U_j,\ \ j=1,\ldots,N$$

where $w\in[0,1]$ is a damping factor chosen to enhance convergence.

The Jacobian matrix entries, $\frac{\partial f_i}{\partial U_j}$, are given by:

$$\frac{\partial f_i}{\partial U_j} = \int_\Omega \left[\tau_r \nabla N_j \cdot \nabla N_i + \frac{q^2 N_C}{\tau_0 k_B T} \mathrm{F}_{-1/2}\left(\frac{F_n - u^k}{k_B T} \right) N_j N_i \right] d\Omega$$

Here, we utilize the identity that governs the derivative of the Fermi-Dirac integral of order k:

$$\frac{d}{dx}\mathrm{F}_k(x) = \mathrm{F}_{k-1}(x).$$

to compute the nonlinearity's contribution to the Jacobian.

Boundary Conditions: At the gate interface, the electrostatic potential is related to the applied gate voltage by the expression:

$$V_G = -V_G + \Phi_G - \psi_{\mathrm{Si}} \qquad (15)$$

Here, V_G denotes the gate bias, Φ_G is the metal work function of the gate electrode, and ψ_{Si} corresponds to the electron affinity of silicon.

At the source and drain terminals, electrically insulating (homogeneous Neumann) boundary conditions are assumed:

$$\frac{\partial V}{\partial n} = 0 \qquad (16)$$

This Neumann-type condition, implying zero normal electric field, is similarly enforced on all remaining boundaries of the simulation domain.

IV. RESULT

The computational domain employed in the simulation is illustrated in Figure 1. A uniform grid resolution of 0.25 nm was utilized along the horizontal x axis, and 0.1 nm along the vertical y axis. The silicon body was modeled with a relative permittivity of 11.7, while the dielectric constant for the oxide region was taken as 3.9.

Concerning electrostatic boundary conditions, the electron affinity of the silicon was assumed to be 4.05 eV, and the metal work function of the two gate electrodes was taken as 4.25 eV. The doping concentration in the source and drain regions was set to $1\times10^{20} cm^{-3}$, while in the channel region, it was reduced to$1\times10^{16} cm^{-3}$.

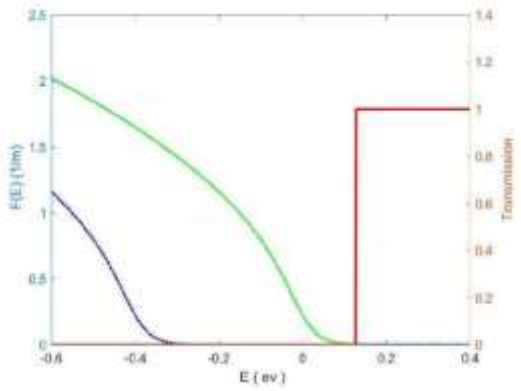

Figure 2: (a) Integrated Fermi functions and transmission coefficient – Iteration 1.

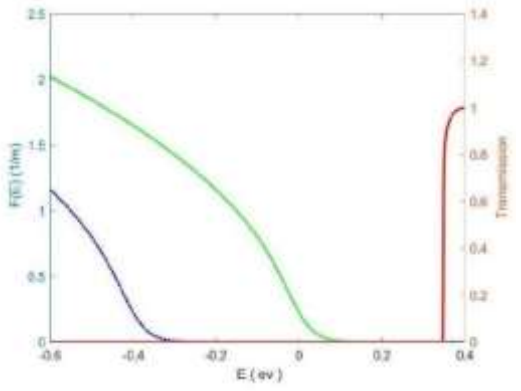

Figure 2: (b) Same quantities at Iteration 10.

In this study, we adopt bulk silicon values for the effective mass: $m_x^* = 0.98m_0$, $m_y^* = 0.18m_0$, and $m_z^* = 1m_0$.

When computing the sub band energy E_{sub}^m, it is assumed that the conduction band edge in the oxide lies 3.34 eV above that of silicon.

Symmetric biasing is applied to the gate electrodes. The source terminal is grounded, implying its electrochemical potential is set to 0 eV, while the drain is biased at 0.4 V.

In Figure 2(a), the integrated Fermi distributions and the transmission coefficient are shown for the condition $V_G = 0.4V, V_D = 0.4V$.

Since the source voltage is fixed, the corresponding Fermi function remains unchanged across iterations. In contrast, the Fermi function at the drain shifts by the drain bias. If $V_D = 0V$, the two Fermi integrals would coincide. In Figure 2(b), the transmission profile exhibits an onset near 0.34 eV, indicating that the tunneling probability remains negligible at early iterations.

Figure 3 presents the evolution of the 2D electron density across iterations for $V_G = 0.4V$, $V_D = 0.4V$. Electron density is observed to vanish at the oxide boundaries, consistent with the imposed boundary conditions. Initially, as shown in Figure 3(a), the potential is uniform, resulting in a relatively flat density profile. In contrast, Figure 3(b) demonstrates that the electron concentration near the source and drain regions has evolved to reflect electrostatic non-uniformities arising from the applied bias.

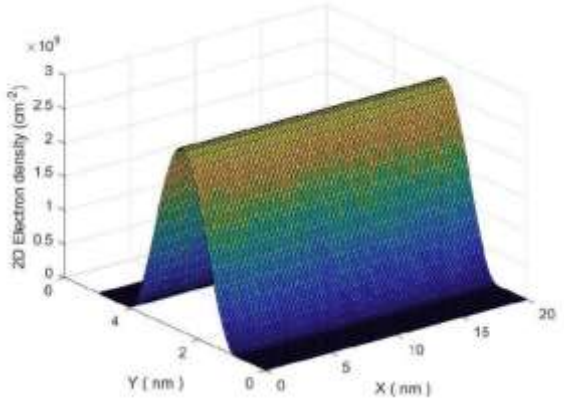

Figure 3: (a) 2D electron density $n_{2D}(x,y)$ -Iteration 1.

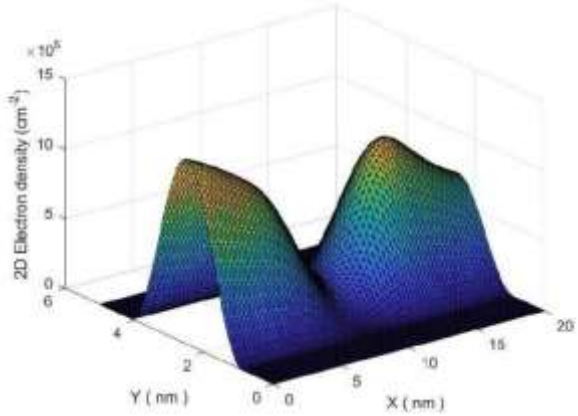

Figure 3: (b) $n_{2D}(x,y)$ at Iteration 10.

IV. CONCLUSION

This study presents a comprehensive simulation framework that integrates the Nonequilibrium Green's Function (NEGF) formalism with the Finite Element Method (FEM) to obtain a self-consistent solution for nanoscale device modeling. An uncoupled mode-space approach is employed to compute the retarded Green's function, which is subsequently utilized to evaluate the electron density. The resulting electron density is then incorporated into the Poisson equation to determine the electrostatic potential distribution.

The nonlinear Poisson equation is solved using the Newton–Raphson iterative scheme, with the computational domain discretized via piecewise linear elements within the FEM framework. Key quantities extracted from the simulation include the spatial distribution of electron density, integrated Fermi levels, and the transmission spectrum.

The obtained results exhibit deviations from the expected physical behavior, indicating limitations in the current modeling approach. These discrepancies suggest the necessity for further refinement of the simulation framework. Future work will focus on improving model fidelity through the optimization of boundary conditions, revision of material parameters, and the implementation of more robust numerical schemes to enhance convergence and predictive accuracy.

References

1. S. Datta, Nanoscale device modeling: the green's function method, Superlattices and microstructures 28 (4) (2000) 253-278.

2. S. Datta, Quantum transport: atom to transistor, Cambridge university press, 2005.

3. L. P. Kadanoff, G. Baym, Q. S. Mechanics, Green's function methods in equilibrium and nonequilibrium problems, Quantum Statistical Mechanics (1962).

4. L. V. Keldysh, et al., Diagram technique for nonequilibrium processes, Sov. Phys. JETP 20 (4) (1965) 1018-1026.

5. R. Venugopal, Z. Ren, S. Datta, M. S. Lundstrom, D. Jovanovic, Simulating quantum transport in nanoscale transistors: Real versus modespace approaches, Journal of Applied physics 92 (7) (2002) 3730-3739.

6. E. Polizzi, S. Datta, Multidimensional nanoscale device modeling: the finite element method applied to the non-equilibrium green's function formalism, in: 2003 Third IEEE Conference on Nanotechnology, 2003. IEEE-NANO 2003., Vol. 1, IEEE, 2003, pp. 40-43.

7. J.-M. Jin, The finite element method in electromagnetics, John Wiley \& Sons, 2015.

8. Z. Ren, Nanoscale mosfets: Physics, simulation and design, Ph.D. thesis, Purdue University (2001).

9. , S. Datta, M. S. Lundstrom, nanomos 2.5: A two-dimensional simulator for quantum transport in doublegate mosfets, IEEE Transactions on Electron Devices 50 (9) (2003) 1914-1925

10. H. Jiang, S. Shao, W. Cai, P. Zhang, Boundary treatments in non-equilibrium green's function (negf) methods for quantum transport in nano-mosfets, Journal of Computational Physics 227 (13) (2008) 6553-6573. ange/13616-fermi}